stellarator news

Published by Fusion Energy Division, Oak Ridge National Laboratory
Building 9201-2; P.O. Box 2009; Oak Ridge, TN 37831-8071, USA

Editor: James A. Rome Issue #11 September, 1990

Around the Labs

Neutral Beam Injection Studies in ATF

Neutral beam heating studies during the current period of operation have emphasized injection into low-density plasmas ($n_e \leq 10 \times 10^{13}$ cm^{-3}). One major goal was to reproduce the W VII-AS results, which have demonstrated that collapses can be avoided during NBI if the ECH operates simultaneously while the electron density is maintained below the cutoff level. A second goal was to obtain the highest possible plasma temperatures with NBI. Beam pulses of 1.5 MW up to 300 ms long were utilized at 1 T without collapses occuring, but there was some evidence that the metal influx from the walls was starting to increase toward the end of the discharges. Electron temperatures did not show the typical, rapid decrease observed when the the electron density is allowed to rise above the ECH cutoff level, but remained close to the pre-NBI values with $T_e(0) \sim 1$ keV. Central ion temperatures typically reached 400 eV, i.e., 100–150 eV higher than previously observed in plasmas which evolved toward a collapse.

Similar experiments have been peformed at 2 T, but so far the operating mode has not been refined enough to avoid collapses, which occur about 100 ms after NBI begins. However, record central ion temperatures for ATF of 1 keV were reached with central electron temperatures of the same magnitude. Figure 1 shows the time history of the O VII ion temperature measured from Doppler broadening of the 1623-Å line. The average radius of this emission is estimated to be at $\rho = 0.2$; most of the signal arises from charge-exchange excitation by the heating beam. The time at which the maximum temperature is attained corresponds closely to the

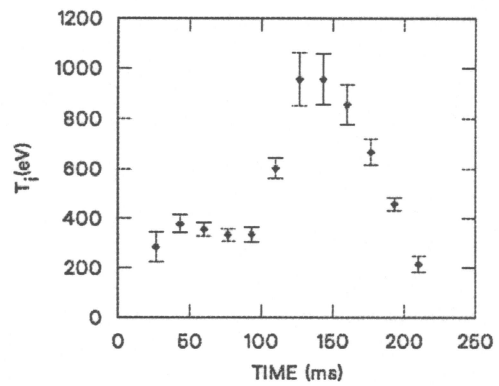

Fig. 1. Time history of the O VII ion temperature in a 2-T, low-density discharge with 1.5 MW of NBI between 200 and 300 ms.

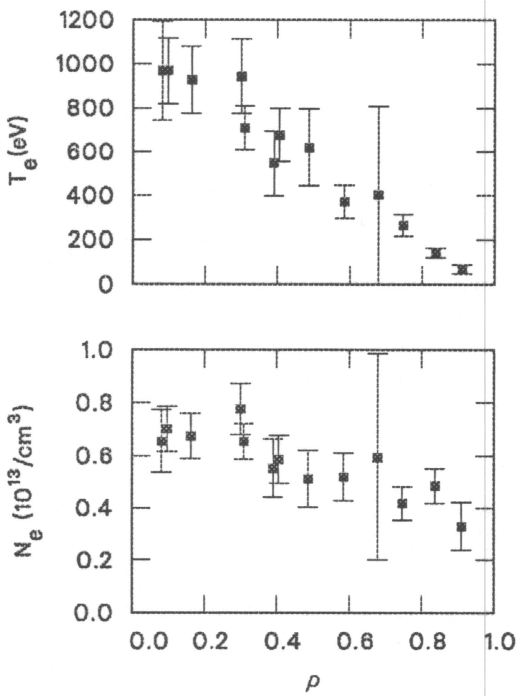

Fig. 2. Electron temperature and density profiles at 135 ms for the plasma characterized by the ion temperatures in Fig. 1.

time at which the stored energy reaches a maximum. Figure 2 shows the radial profiles of T_e and n_e obtained by Thomson scattering at the time when the ion temperature is 1 keV. The more or less triangular electron temperature profile and the very broad electron density profile are typical of many ATF operating conditions.

Ralph Isler for the ATF Team
Oak Ridge National Laboratory
P.O. Box 2009, MS 8072
Oak Ridge, TN 37831-8072, USA

Progress on Wendelstein VII-AS with NBI

During July 1990 the investigations at Wendelstein VII-AS were concentrated on experiments with neutral beam injection (NBI). After carbonization by glow discharges with a mixture of He and 30% CD_4 (CH_4), the content of high-Z material (Fe and Ti) was significantly reduced. With reduced radiative losses the parameter range of plasmas was extended to much higher densities (n_{e0} up to 2.5×10^{20} m^{-3}), for a pulse duration up to 300 ms. The target plasma is produced by 70-GHz ECRH at values of the main field $B = 2.5$ or 1.25 T. Up to the full power of 1.5 MW of NBI was used for further heating, injecting H^0 with an accelerating voltage of 45 kV. With carbonized walls the recycling coefficient is greater than one, and the evolution of the discharge is characterized by a steady increase of density. Typically, the rate of density increase is determined by a ratio of one to three for the particle flux associated with the neutral injection and the gas released from the wall. Using He glow discharges and reducing the input power allowed us to stabilize the density close to $n_{e0} = 1 \times 10^{20}$ m^{-3}.

The maximum energy content achieved in Wendelstein VII-AS so far was 28 kJ at 1.3 MW absorbed power, and the averaged beta was 0.62% with an axis value of 1.4% for a field of 2.5 T, at an average plasma radius of 0.17 m and a rotational transform of 0.34. At densities of about 2×10^{20} m^{-3} electron temperatures of 0.6 keV were measured. With balanced injection a bootstrap current of 1 kA was observed. Ion temperatures could not be measured at these high densities since the diagnostic beam and the CX flux from the center were completely absorbed. At lower densities of ~10^{20} m^{-3}, peak temperatures for electrons T_{e0} of about 0.75 keV and for ions T_{i0} of about 0.6 keV were achieved, see Fig. 1, with a maximum energy replacement time of about 20 ms.

Operating Wendelstein VII-AS at low field, $B = 1.25$ T, allows us to maintain discharges at similar densities n_{e0} ~10^{20} m^{-3} and slightly reduced temperatures. Using only three injectors (P_N below 1.1 MW) yields plasmas with an averaged beta of 0.65% and an energy replacement time of typically 10 ms. The maximum obtainable density and consequently beta seem to be related to the absorbed power, as long as the electron temperature stays above 350 eV to minimize the radiative losses and prevent a radiative collapse.

Presently the device is open for maintainance, modification of the diagnostics, and installation of the 140-GHz launching system. After the IAEA meeting in October 1990 the experiments will continue. Based on the experience at other devices, the planned boronization may improve the situation and partly help to eliminate the remaining problems of recycling control and the need to further reduce oxygen and carbon contamination.

H. Renner for the W VII-AS Team
Max-Planck Institut für Plasmaphysik
Association EURATOM-IPP
D-8046 Garching, FRG

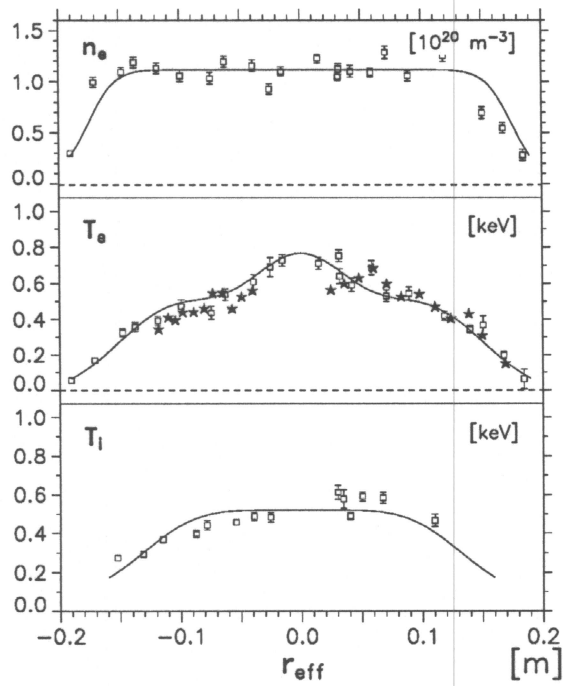

Fig. 1. Electron density, electron temperature, and ion temperature profiles versus effective plasma radius for pure NBI heating. n_e and T_e from Thomson scattering, T_e(★) from ECE, and T_i from active CX neutral particle analysis.

Efficiency of Electron-Cyclotron Plasma Heating on the L-2 Stellarator

Experiments using ECR heating of a current-free plasma in the L-2 stellarator have shown that this technique makes it possible to produce a plasma with $T_e(0) =$ 1 keV, $n < 2 \times 10^{13}$ cm^{-3}, $T_i(0) = 0.1$ keV, $\beta(0) = 0.5\%$, and $\tau_E = 3$ ms. According to calculations, the absorption of microwave power for such a plasma amounts to approximately 90%, whereas the absorbed power P_{ab} measured from the jump of the diamagnetic derivative did not exceed 50–60%. The measurements of microwave absorption have shown that the damping length does not exceed 10% of the device perimeter, and in the resonance conditions all the power is absorbed. Such an anomalously low absorption of microwave power according to diamagnetic measurements was observed in the case of two different types of microwaves: the ordinary wave at the fundamental harmonic ($\Omega = \Omega_{ce}$) and the second harmonic of the extraordinary wave ($\Omega = 2\Omega_{ce}$).

In this article the method for measuring the absorbed power from the plasma diamagnetism is analyzed. It is well known that this method is based on the energy balance equation

$$dW/dt = P_{ab} - P_c - P_{rad} - P_{cx}$$

where W is the total plasma energy, P_c is the thermal conductivity flux, and P_{rad} and P_{cx} are the radiative and charge-exchange losses. When the microwave power is terminated, we assume all the losses to remain constant at this moment of switching off. The change of the plasma energy derivative amounts to P_{ab}. The assumption of constant P_{rad} and P_{cx} is clear from direct measurements of these magnitudes and that of constant P_c follows from the measurements of the plasma boundary parameters which are heated by thermal conductivity. The dynamics of W were determined by diamagnetic loops.

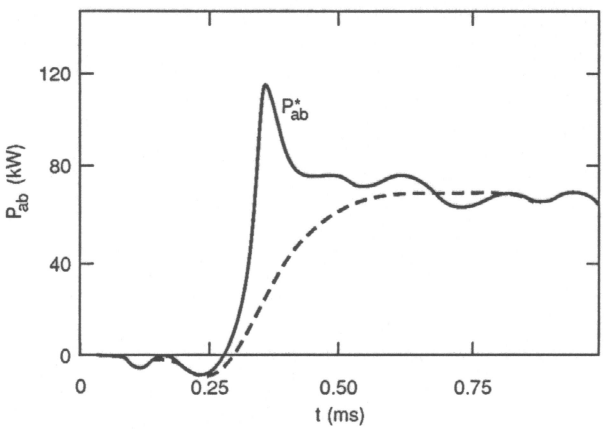

Fig. 1. Time evolution of the derivative of diamagnetic signals close to the moment when the microwave power is switched off.

To determine correctly the derivative of the diamagnetic flux, it is necessary to take into account the effect of the conducting vacuum chamber. In our case this can be done by a simple correction formula

$$\left(\frac{d\Phi}{dt}\right)_{true} = \left(1 + \tau_{chamber}\frac{d}{dt}\right)\left(\frac{d\Phi}{dt}\right)_{measured}$$

which allows us to find the true magnetic flux time derivative when we know the measured one. The time constant $\tau_{chamber}$ is in our case 105–110 μs. It was evaluated both experimentally and theoretically. Here we illustrate the importance of incorporating an auxiliary term

$$\tau_{chamber}\frac{d}{dt}\left(\frac{d\Phi}{dt}\right)_{measured}$$

for determining the absolute magnitude of the derivative jump, using as an example the experiments on plasma heating at the second harmonic ($\Omega = 75$ GHz, $B = 1.34$ T, $P_0 = 200$ kW).

After breakdown, the plasma density becomes quasi-stationary for up to a time less than 1 ms and the electron temperature and plasma energy are quasi-stationary for up to 4–5 ms. The conventional diamagnetic measurements showed that at the beginning of the discharge the magnitude P_{ab} is noticeably higher than in the quasistationary phase. This peculiarity in the behaviour of P_{ab} is typical for almost all of the heating regimes which differ by the magnitudes of plasma density, the levels of introduced power, and the types of waves applied for heating. Figure 1 shows the time evolution of the derivative of diamagnetic signals close to the moment when the microwave power is switched off (the decay time of the power is up to 50 μs). In the same figure there are given the results of processing this signal incorporating the effect of the conducting chamber. It is seen that the true magnitude of the derivative jump (it is P^*_{ab} in figure) is in this case 40% higher than measured one. What does this difference mean? Such a picture should be observed in the case when there is a certain fraction of plasma with a rather small lifetime energy value (less than or comparable to the $\tau_{chamber}$ value). This short-lived fraction cannot be detected because of the conducting chamber integration effect. The energy lost from the plasma during the fast decay phase does not, as a rule, exceed 5–7% of the whole plasma energy. However, the gain P_f of the absorbed power, taking this

phase into account, could in some cases be fairly noticeable. As a rule, an essential difference between P_{ab} and $P^*_{ab} = P_{ab} + P_f$ is observed in a quasistationary phase of the discharge only, as illustrated in Fig. 2. This figure shows the time evolution of magnitudes P_{ab} and P_f during the heating pulse when the launched power was $P_0 = 200$ kW. It is seen that P_f (the microwave power absorbed by the short-lived plasma component) at the end of the heating pulse amounts to 30 kW. It is of interest to note that the total absorbed power remains practically constant throughout the heating. This may be because the processes of power absorption by thermal and short-living components are competing. The role of this component in the total plasma energy balance is more important and the level of the launched power is increased as the plasma density is decreased. Figure 3a shows the dependence of P_{ab} and P_f on density at $P_0 =$ 200 kW, and Fig. 3b shows their dependence on input power at $n = 1 \times 10^{13}$ cm^{-3}. Figure 3c gives the dependence of the absorption coefficient $\eta = P^*_{ab}/P_0$ on the magnitude of the input power. This dependence is seen to be weak, and the absolute magnitude of η does not exceed 60%.

Thus, we have a substantial discrepancy in the absolute values of absorbed power being measured from the microwave damping and diamagnetism. To understand this discrepancy we may assume the following picture. The fast energy decay phase could be associated with the fast and trapped electrons being localized mainly in the region of microwave injection, and rapidly escaping this region. The diamagnetic loops are nonuniformly situated along the perimeter of the torus, and in the nearest vicinity of microwave injection these loops do not exist at all. It may be thus expected that the measured energy derivative jump may not include all the power absorbed by these trapped electrons.

Conclusions

The analysis of diamagnetic measurements during microwave plasma heating in the L-2 stellarator allowed us to discover the existence of a short-lived plasma component which can absorb a noticeable fraction of the input power. The energy stored in this component is a fairly small part of the total plasma energy. This analysis indicates also that for diamagnetic measurements of fast processes it is necessary to take into account the effect of the conducting chamber, which may distort essentially the measured signals.

Oleg I. Fedyanin
Institute of General Physics
Moscow, USSR

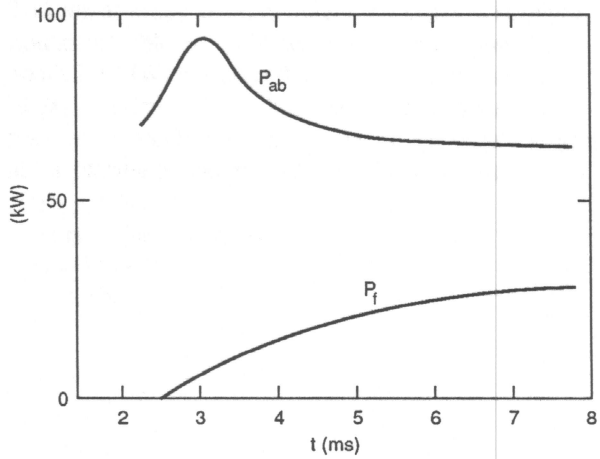

Fig. 2. The two components of P^*_{ab}.

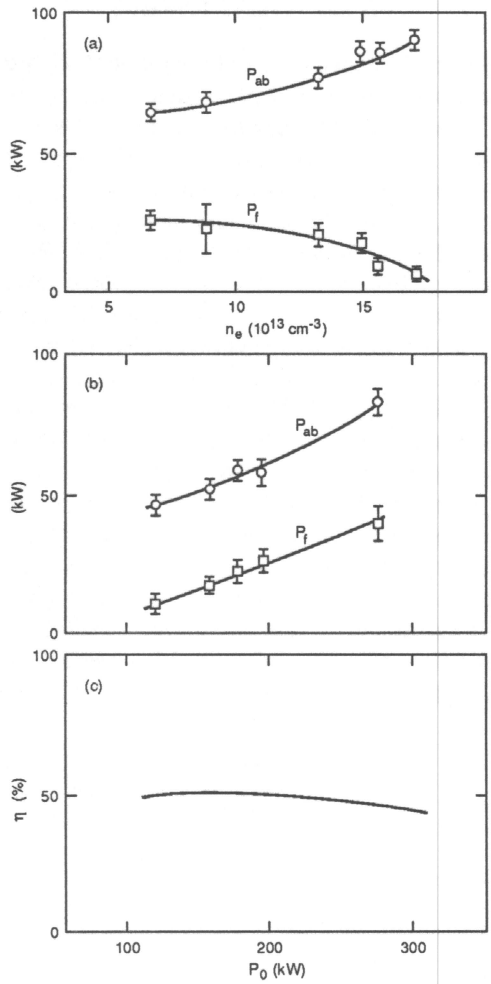

Fig. 3. (a) Dependence of P_{ab} and P_f on density at $P_0 = 200$ kW. (b) Dependence of P_{ab} and P_f on input power at $n = 1 \times 10^{13}$ cm^{-3}. (c) Dependence of absorption coefficient $\eta = P^*_{ab}/P_0$ on the magnitude of the input power.

Status of URAGAN-2M Physics Studies

URAGAN-2M (Cyrillic abbreviation Y-2M) is the new device under construction at the Kharkov Institute of Physics and Technology in the USSR [1]. The design value of the magnetic field is $B_0 = 2$ T, the major radius of the system is $R_0 = 1.7$ m, and the plasma aspect ratio is about 10. Y-2M is a torsatron with $m = 4$ field periods and predominant $l = 2$ symmetry.

Each of the two helical windings is divided into two split helices. The helical windings are modulated so as to increase the magnetic ripples in the weak field strength region on the outside of the torus. The major part of the toroidal field is produced by a set of 16 circular coils. The two systems of vertical field coils consist of four pairs of compensation windings that compensate the transverse magnetic field $B_\perp$ from the unidirectional helical winding currents by the use of oppositely directed currents and by two pairs of correction windings with positive or negative currents. The latter pairs of windings provide more refined control of the position and shape of the magnetic surfaces and of the size of the last closed magnetic surface.

The magnetic configuration

Depending on the current ratios in the four coil systems, the size of the last closed magnetic surface and the radial profiles of the rotational transform, ι, and of the specific magnetic volume $V'/V'(0)$ are changed. For convenient classification of the configurations two parameters are used: $k_\varphi = B_{\varphi,h}/B_0$ and $B_\perp/B_0$, where $B_{\varphi,h}$ is the toroidal component of the helical windings at the major radius position R_0, and $B_0 = B_{\varphi,t} + B_{\varphi,h}$ is the averaged total toroidal field at R_0. $B_\perp$ is the resulting transverse correction field at R_0.

For our detailed study now we have chosen three types of configurations:

A. $k_\varphi = 0.375$ and $B_\perp/B_0 = 2.8\%$
B. $k_\varphi = 0.375$ and $B_\perp/B_0 = 1.5\%$
C. $k_\varphi = 0.295$ and $B_\perp/B_0 = 2\%$.

Configuration A is considered as one of the working regimes for URAGAN-2M with an averaged radius $\langle a \rangle \approx 17$ cm, $\iota(0) \approx 0.55$, and $\iota(a) \approx 0.75$, this is the so-called standard case. Configuration B has the same averaged plasma radius, which is limited as in the previous case by resonance value $\iota = 4/5$; the rotational transform on axis $\iota(0) = 0.44$. The third configuration has a larger radius of the last closed magnetic surface $\langle a \rangle \approx 25$ cm and smaller rotational transform $\iota(0) = 0.33$ and $\iota(a) \leq 0.5$. This configuration may be used in a modification (new version) of URAGAN-2M which would have a profiled vacuum chamber.

The suppression of magnetic islands

During preliminary computations of magnetic surfaces, magnetic islands at $\iota = 4/6$ were discovered in the Standard case [2] which limited the averaged radius of the last magnetic surface to 12 cm. With help from the Wendelstein VII-X group at the Max-Planck Institut für Plasmaphysik (IPP), Garching, one way has been found to suppress these magnetic islands: changing the second modulation coefficient in the helical winding law from -0.0171 to +0.0070 can reduce the magnetic islands from 2–3 cm to 0.3 cm [3].

After that another way has been found [4] to suppress the magnetic islands at $\iota = 4/6$. Almost the same effect is obtained by employing special values for the poloidal conductor currents.

Eliminating the islands from the configuration will enable us to study physics for a configuration with an averaged magnetic surface radius not less than 17 cm.

Particle orbits

Charged particle trajectories obtained by integration of the guiding center equations have large deviations from a magnetic surface, which are characteristic for the motion of helically trapped particles with an unfavorable modulation of the magnetic fields. However, the radial drift of helically trapped particles may be considerably compensated by a radial electric field of the correct sign to increase the poloidal velocity of these particles. Computations confirmed the adiabatic conservation of the longitudinal invariant $J_\parallel = \oint v_\parallel dl$.

Velocity space loss regions

We are now studying the loss regions using the guiding-center approximation with an idealized magnetic field model that takes into account the basic toroidal and helical harmonics and the nearest sidebands of the basic helical harmonics. We have shown that the loss regions in velocity space are larger than for the conventional $l = 2$ stellarator because of satellite harmonics with the same sign as that of the main helical harmonic, but an electric field of the sign which gives the physical effect mentioned above, decreases the loss regions [5].

Wendelstein VII-X Engineering Studies

Engineering design for Wendelstein VII-X is a challenge in a number of new fields. Essential tasks are the development of the superconducting modular coil systems, their coil housings and the common support structure, integrated into the modular cryostat. Guidelines for these tasks have been worked out. Close contact with industry is essential. A co-operation exists between IPP Garching and KfK Karlsruhe in the field of fusion technology. Ongoing work has been documented in pertinent conferences. Five contributions will be presented by members of the stellarator group at IPP Garching at the forthcoming 16th Symposion on Fusion Technology (SOFT), to be held at the Queen Elizabeth Conference Centre, Westminster, London, UK, September 3–7, 1990. Information on these papers follows.

J. Sapper et al.

The Stellarator Wendelstein VII-X, Technical Design and Engineering.

Optimization of the HELIAS configuration (HELIcal Advanced Stellarator) chosen for Wendelstein VII-X has yielded a plasma aspect ratio of 10. The plasma physics objectives require powerful plasma heating in the range 10 to 25 MW, an adequate field strength up to $B_0 = 3$ T, and sufficient distance between the plasma and first wall. This has led to the choice of a major radius $R_0 = 5.5$ m for Wendelstein VII-X. A superconducting magnet system is chosen because of reactor-relevant aspects, and an estimated heating pulse duration of typically 10 to 20 s to achieve quasi-steady-state plasma operation. Normal conducting Cu-coils would allow a flattop time of up to 5 seconds only; the required electric power and energy significantly exceed the existing power supply of IPP.

Wendelstein VII-X utilizes two independent modular coil systems, 50 non-planar coils with five different coil shapes for the standard configuration, and an additional set of 20 planar coils with two different shapes for parameter variation (iota, axis position, shear, etc.). The winding pack cross section of the non-planar coils amounts to 18×21 cm^2. A total current of 1.76 MA is required for the design field of 3 T. The NbTi cable-in-conduit conductor with forced-flow cooling measures approximately 1.6 by 1.6 cm^2; there are about 120 turns. The modular cryostat encases both coil systems. Its inner surface serves as vacuum envelope of the plasma volume of 30 m^3. The cold mass amounts to about 350 tons, i.e., it is comparable to that of the Large Coil Task (LCT). A refrigeration power of 4 to 8 kW at 4 K temperature is envisaged. The realization of the project will be in two essential steps, a prototyping phase of about three years will be followed by a manufacturing phase of four years, ending with one additional year for final assembly.

J. Kißlinger et al.

Magnetic Field and Coil Systems of the Modular Helias Configuration HS 5-10.

The Helias coil system HS5-10 has been selected as reference configuration for the development of Wendelstein VII-X. Its magnetic fields have optimized plasma confinement and MHD-equilibrium properties, and offer the prospect of stable plasma operation between 4 and 5%, depending on heating and transport. An important design criterion in Wendelstein VII-X is poloidally closed coils for the magnet system. The coils are calculated after the plasma equilibrium has been specified. This procedure differs from the conventional approach, where the coil system is optimized and the plasma behaviour is investigated afterwards. The surface current distribution for the modular coils is determined iteratively, using the NESCOIL-code to obtain spatial current distributions, and the GOURDON field tracing code. The coils are optimized according to the following criteria:

- maximum distance towards the plasma maximum distance between two adjacent coils
- maximum radius of curvature at their corners
- quality of the resulting magnetic field with respect to the originally given field.

The last point also includes the reduction of magnetic islands on magnetic surfaces with low order rational values of the rotational transform. Geometrical data of the coils are listed in Table I.

TABLE I : Characteristic data of the Helias configuration HS5-10.

Average major radius	R_0	5.5 m
Average plasma radius	a	0.54 m
Average coil radius	r_c	1.14 m
Radial coil height	t	0.21m
Lateral coil width	w	0.18 m
Average coil volume	V_c	0.29 m^3
Total coil volume	$n\,V_c$	14.5 m^3
Min. radius of curvature	ρ_c	0.27 m
Coil number total	n	50
Coil number per FP	n_p	10
Total coil current	I_c	1.76 MA
Overall current density	j_{av}	46.6 MA/m^2
Stored magnetic energy	W	0.6 GJ
Induction on axis	B_0	3.0 T
Min. distance plasma-wall	Δ_{pw}	0.11m
Distance coil to wall	Δ_{cw}	0.18 m
Min. coil center distance	Δ_{cc}	0.26 m

This coil-system provides nested magnetic surfaces and a helical axis. In the standard configuration the rotational transform on axis is $\iota(0) = 0.84$ and about 1 at the edge. In Wendelstein VII-X experimental flexibility is achieved by additional planar coils with individually adjustable currents. They allow to introduce toroidal and vertical fields as well. A broad range of magnetic field variations is thus possible, while maintaining a magnetic well and emphasizing specific features of the Helias field:

- variation of the rotational transform by ± 20%
- shift of the magnetic axis by about ± 5 cm
- variation of the magnetic mirror ratio
- variation of shear, e.g. introducing edge values between $\iota(a) = 5/5$ and 5/4 for $\iota(0) = 0.91$.

Characteristic vacuum field data of the different field configurations are calculated, such as the rotational transform, shear, magnetic well, variation of |B| on the magnetic surface, the ratio of parallel and perpendicular current density, and geometrical factors which enter relationships for neoclassical transport or the bootstrap current. The modular coils developed for Wendelstein VII-X sufficiently approximate the given Helias configuration, fulfil technical constraints, offer space between plasma and first wall, and leave access to the plasma. Magnetic islands in the edge region are of potential use as divertors. Novel trim coils allow to adjust their size and phase.

J. Simon-Weidner et al.

On Mechanical Stresses in Large Helias Coil Systems and the Influence of Contact Effects

Studies of electromagnetic forces and the associated stresses in the coil winding packs and their support have been published for various earlier coil sets and their support. This paper concentrates on the reference configuration of Wendelstein VII-X. Net coil forces, up to 4 MN with horizontal and vertical components, and local force densities in the coils are obtained by the EFFI code. The current density averaged over the winding pack is 48 MA/m^2; local peak fields at the coil are 6.1 T. These values are well in the operation regime of NbTi as superconductor at 4 K temperature. The support system consists of individual coil housings, connected by a common vault. One field period is treated simultaneously. Using orthotropic material data of the EURATOM-LCT coil, and assuming a rigid contact between the coils and their housing, yields for the winding pack of a typical coil, i.e. coil No 3 of the modular system, local maximum values of 32 MPa for the equivalent stress, and below 20 MPa for the shear stress. The influence of an assumed symmetric gap between the winding pack and the housing of one of the 10 coils is also investigated.

E. Harmeyer et al.

Force and Stress Calculations for a Non-Planar W VII-X Demonstration Coil

Among the key elements of the engineering tasks for Wendelstein VII-X are the construction and test of a demonstration coil. The coil No 3 of the modular system has been selected because of its rather large toroidal excursions, accompanied by a finite indentation. As test bed we consider the TOSKA facility at KfK Karlsruhe, a large cryostat which uses the EURATOM-LCT coil as background field. In the first part of the study the relative orientations of these two coils were arranged such as to introduce the local peak field of 6.1 T of the Wendelstein VII-X standard case at a certain position of the demonstration coil. The coil is supported by a stainless steel housing and connected to the LCT coil by four columns and an intermediate plate. The support elements were determined in the second part of the investigation. As a result of several iterations nearly the same maximum values of the equivalent stress and slightly larger ones of the shear stresses are calculated for the winding pack of the demonstration coil in the test, as were found for the standard case of the toroidal Wendelstein VII-X field, although the spatial distributions of the electromagnetic force densities, and, consequently, of the stress components differ for both cases. These computations are done for the design current in the demonstration coil, and for a reduced current in the LCT coil. Therefore overload tests are also possible.

O. Jandl et al.

FE Modelling with Sliding Effects Compared to Measurements Obtained from the Non-Planar Coils for the Stellarator VII-AS

The Advanced Stellarator Wendelstein VII-AS had shown some unexpected local displacements of certain coils during initial operation at fields of 2.5 T, which caused excessive stress in the insulation. Therefore the FE model, originally MSC/NASTRAN, has been re-activated and converted to new data sets for the ANSYS code. Calculations of stresses and displacements were done for half of a field period of the coils and their supporting elements. Parametric studies of the gap widths are performed for the coil of interest with refined supporting elements. By the end of 1989 the support of these coils had been improved; since February 1990 Wendelstein VII-AS was operated satisfactorily under full field for about 3700 shots.

F. Rau for the W VII-X Team
Max-Planck Institut für Plasmaphysik
Association EURATOM-IPP
D-8046 Garching, FRG

The summertime always coincides with an increase in personnel exchanges among the various stellarator laboratories. Such exchanges play an important role in the cross-fertilization of ideas and the exchange of knowledge and techniques.

At Max Planck Institut für Plasmaphysik

Allen H. Boozer worked as an External Scientific Member of IPP in the theory group of A. Schlüuter and J. Nührenberg between June 1 and July 31.

A number of guests worked with the Wendelstein VII-AS Team in 1990 and are co-authors of the invited paper at the 17th European Conference in Amsterdam:

Shaofeng Jiang, from Southwestern Inst. of Physics, Leshan, China, since 14 October 1988.

Hideki Zushi, from Plasma Physics Laboratory, Kyoto University, Japan, between 3 February and 29 April.

Macarena Liniers and **Maria-Anna Ochando**, from CIEMAT, Madrid, Spain, between 1 April and 30 June.

N. Bezedin and **A. Gutarev**, from Inst. of Physics and Technology, Kharkov, USSR, between 29 April and 27 May.

Valeriy I. Afanasiev, from Ioffe Institute, Leningrad, USSR, since 15 July, and until 14 October.

At Oak Ridge National Laboratory

This summer a group of scientists from CIEMAT (Madrid, Spain) worked on ATF in a continuation of a longstanding collaborative effort.

Carlos Hidalgo has been involved in the ATF edge fluctuation studies since July 1989, in the framework of the collaboration between ATF, CIEMAT, and TEXT (Austin, Texas). The near-term emphasis of his research on ATF is the study of the scaling properties of the edge turbulence and transport, temperature fluctuations, and velocity shear layer.

Maria Ochando is collaborating on the global energy balance studies using spectroscopy and bolometry as basic techniques.

Beatriz Brañas and **Joaquin Sanchez** are involved in fluctuation studies using microwave reflectometry. Present efforts are focused on the determination of coherence lengths, with emphasis on the location of large coherence density structures in the gradient region of ATF.

Alexander Shishkin of the Kharkov Institute of Physics and Technology and **Oleg Fedyanin** of the Institute of General Physics in Moscow visited ORNL for three weeks in July and August. Dr. Shiskin worked with the MHD Theory group to characterize the expected MHD characteristics of the Y-2M torsatron and to study the possibility of using the Y-2M poloidal coil set to improve the outer flux surfaces.

Dr. Fedyanin worked on improving the interpretation of magnetic stored plasma energy measurements in ATF and the interpretation of ECH and NBI heating results.

During July and August, **Shoichi Okamura** from the National Institute for Fusion Science, Nagoya, worked with the ATF team to understand the similarities and differences between NBI in ATF and CHS.